frontiers | Frontiers in Environmental Science

TYPE Original Research
PUBLISHED 07 December 2022
DOI 10.3389/fenvs.2022.1083616

Check for updates

OPEN ACCESS

EDITED BY
Bao-Jie He,
Chongqing University, China

REVIEWED BY
Benyamin Khoshnevisan,
University of Southern Denmark, Denmark
Chunye Lin,
Beijing Normal University, China

*CORRESPONDENCE
You Li,
liyou@igsnrr.ac.cn

SPECIALTY SECTION
This article was submitted to Water and Wastewater Management, a section of the journal Frontiers in Environmental Science

RECEIVED 31 October 2022
ACCEPTED 23 November 2022
PUBLISHED 07 December 2022

CITATION
Li H, Liao X, Li Y, Liu Q and Luo J (2022), Insight into the degradation mechanism of fluorene by ferrous/humic acid activated persulfate: Free radical reactions, functional group verification and degradation pathway.
Front. Environ. Sci. 10:1083616.
doi: 10.3389/fenvs.2022.1083616

COPYRIGHT
© 2022 Li, Liao, Li, Liu and Luo. This is an open-access article distributed under the terms of the Creative Commons Attribution License (CC BY). The use, distribution or reproduction in other forums is permitted, provided the original author(s) and the copyright owner(s) are credited and that the original publication in this journal is cited, in accordance with accepted academic practice. No use, distribution or reproduction is permitted which does not comply with these terms.

Insight into the degradation mechanism of fluorene by ferrous/humic acid activated persulfate: Free radical reactions, functional group verification and degradation pathway

Haonan Li[1,2,3], Xiaoyong Liao[1,2], You Li[1,2]*, Qiongzhi Liu[1,2,3] and Junpeng Luo[1,2,3]

[1]Key Laboratory of Land Surface Pattern and Simulation, Institute of Geographic Sciences and Natural Resources Research, Chinese Academy of Sciences (CAS), Beijing, China, [2]Beijing Key Laboratory of Environmental Damage Assessment and Remediation, Beijing, China, [3]University of Chinese Academy of Sciences, Beijing, China

This study evaluated the performance of humic acid (HA)/ferrous ion (Fe (II)) activating persulfate (PS) for fluorene (FLU) degradation. Results showed that HA/Fe(II)/PS system exhibited the best performance for PS activation to eliminate FLU. Compared to the non-activated case, the degradation efficiency of FLU had increased by 37%–43% in HA activated PS system. HA had significant synergistic effects on Fe (II) activated PS process, but ferric ion (Fe(III)) inhibited the degradation. We confirmed that semiquinone radical ($SQ\cdot^-$) acted as the dominant activating group by quenching and electron spin resonance (ESR) experiments, which promoted more radicals generated. The proportion of benzoquinone (BQ) and Fe(II) wielded a considerable influence on FLU degradation, and the optimal concentration ratio was 1:1. Four possible degradation pathways of FLU were deduced, involving ring-opening of the aromatic ring, decarboxylation, oxidative dehydrogenation and hydroxylation.

KEYWORDS

humic acid (HA), persulfate activation, fluorene, free radicals, degradation mechanism

Introduction

Polycyclic aromatic hydrocarbons (PAHs) act as common hazardous contaminants, which are widely distributed throughout the sediments and groundwater. The worldwide discharge of PAHs has aroused wide public concern because of their highly lipophilic, bio-accumulative and highly toxic (Rombola et al., 2015; Drwal et al., 2019). Nam et al. (2015) conducted a series of toxicity tests on Fluorene (FLU), Anthracene, Phenanthrene, Fluoranthene, and Pyrene through earthworm experiments. Results showed that only FLU and Phenanthrene took on great toxicity which could cause cancer, abnormality and sudden change (Nam et al., 2015). Besides, the heterocyclic derivatives (O-PAHs, S-PAHs

and N-PAHs) of FLU have strong persistence and higher toxicity than the parent, and the environmental risk may be seriously underestimated (Hayakawa, 2016; Ding et al., 2019).

Persulfate (PS) oxidation is considered as an emerging advanced technology for recalcitrant organic compounds, with the advantages of a long half-life period and high reactivity (Dong et al., 2017; Li et al., 2017; Zhou et al., 2018; Yousefi et al., 2019; Zhou et al., 2019). But PS needs to be activated to maintain powerful oxidization by producing free radicals, including sulfate radical ($SO_4^{\cdot-}$) and hydroxyl radical (OH). Various strategies for PS activation have been proposed including transition metal ion (Liu et al., 2020; Xiao et al., 2020), heating (Wang et al., 2017), alkali (Qi et al., 2016; Garcia et al., 2022), photocatalysis (Liu et al., 2017) and carbon-based materials (Liu et al., 2022). Among the varied approaches, scientists are seeking to establish a more environmental and cost-effective activated method for PS.

Humic acid (HA) is a kind of complex polymer containing carboxyl, alcohol hydroxyl, phenolic hydroxyl, carbonyl, quinone and other functional groups, as well as many aromatic ring conjugated structures and unstable free radicals (Duesteberg and Waite, 2007; Kang and Choi, 2009; Sun et al., 2016). Recently, HA has been demonstrated as a potential activator for PS, with the advantages of biocompatibility, sustainability, and environmental friendliness, but the limited catalytic performance hindered its further applications (Xu et al., 2022; Yao et al., 2022). UV-visible analysis showed that the π electron in HA strongly affected DNT degradation, and the complexation between HA and Fe(II) could promote the degradation process (Li et al., 2019). Besides, a cyclic reaction may happen between quinones and Fe(II), which can promote the generation of more active species, thus improving the degradation effect of contaminants (Leng et al., 2014). To sum up, combining HA and iron-based catalysts may be a feasible idea for PS activation to eliminate FLU from environmental substances.

The dosages and proportion of various activators are crucial for toxic recalcitrant organic pollutants degradation. Studies have shown that small quantities of HA can enhance the degradation rate of trichloroacetic acid (TCA), but excessive HA will be consumed unproductively with $SO_4^{\cdot-}$ and OH, resulting in a lag period of degradation (Westerhoff et al., 2007; Li et al., 2013). The reactivity of quinones in HA is in connection with the REDOX cycle, including the reversible paths between quinones and semiquinone radicals. Research has found that the degradation performance of activated PS was greatly improved by adding quinones (Leng et al., 2014). The removal of 2,4,4′-trichlorobiphenyls (PCB28) has reached 88% by quinones activated PS, while the degradation efficiency of single PS and quinones system is only 20% and 9% respectively (Fang et al., 2013). Therefore, it is important to figure out the feasibility of HA combined with Fe for PS activation in PAHs degradation. Moreover, the involved mechanisms including degradation products and the complete degradation pathway of PAHs need to be further systematically studied.

To achieve the above goals, FLU was selected as representative PAHs in this study. The coupling of HA and Fe (II) for PS activation in degradating FLU was systematically studied and crucial parameters on oxidation properties were explored. The key active species and functional groups were investigated by quenching experiments, characterization analysis and electron spin resonance (ESR). Moreover, the degradation products and environmental risks were analyzed and evaluated, then possible degradation pathways were proposed. The work can provide novel insights into the oxidation mechanism of FLU by HA activated PS.

Materials and methods

Materials

All chemicals used in this study were analytical grade or higher. Sodium PS ($Na_2S_2O_8$, >99%), ferrous sulfate ($FeSO_4$, >99%), Ferric sulfate ($Fe_2(SO_4)_3$, >99%), HA (>90%), 1,4-benzoquinone (BQ), anhydrous sodium sulfate, silica gel, n-hexane (95%, HPLC grade), dichloromethane and acetone (99.9%, HPLC grade) were purchased from China National Pharmaceutical Group Corporation. The standard PAH samples were purchased from the National Center for Standard Substances. All solutions were prepared using deionized water (18.2 MΩ cm^{-1}).

Degradation kinetics experiment

A series of batch experiments were carried out at room temperature. Four treatments were set up in the experiment, including HA/Fe(II)/PS, HA/PS, Fe(II)/PS and PS alone, respectively. In detail, a set amount of FLU solution (15 mM, 10 ml), 10 ml of catalysts ($FeSO_4$, 0.5 M; HA, 0.5 M) and a certain amount of PS (0.5 M, 10 ml) were all added into a 100 ml conical flask. Then they were mixed in a constant temperature incubator shaker (25°C) at 150 rpm for 24 h. The samples were collected within a preset time (5 min, 10 min, 20 min, 30 min, 1 h, 2 h, 4 h, 8 h, 16 h and 24 h), and immediately terminated the reaction process by adding anhydrous ethanol in tiny quantities. The samples were collected and filtered through 0.45 μm PTFE membranes at a predetermined time, then they were stored in a refrigerator at 4°C for further analyses. After filtration, extraction, purification and condensation, the concentrations of FLU were determined. Results showed that the recoveries of all treatments were in the range of 89.8%–95.1%. Besides, the relative deviations of FLU concentrations in all parallel treatments were less than 10%. The reproducibility of the

measurements was determined in triplicates and then mean value was calculated.

EPR experiments

In order to evaluate the feasibility of HA combined with iron in PS activation, the key parameters were systematically analyzed. Benzoquinone (BQ) was choosn as the representative active substance in HA to explore the free radical process of synergistic activation of PS with Fe (II). In a typical experiment, the concentration of PS is fixed at 5 mm, the concentration of DMPO is 0.1 mm, and various dosages of BQ, Fe (II) and Fe (III) were set up. The variables had been combined to examine the free radicals of the PS oxidation system. Briefly, all the reagents or solution were quickly put into the centrifuge tube and determined on site.

Analytical methods

The pre-treatment processes, analytical methods and determining techniques for PAHs had been described elsewhere (Li et al., 2019). FLU in the reaction solution was extracted with 10 ml dichloromethane three times at 250 r min^{-1} for 10 min. The extraction solutions were collected in an eggplant bottle. Subsequently, it was concentrated to 0.5 ml by a rotary evaporator and diluted with n-hexane to constant volume (1 ml). The samples were determined by gas chromatography-mass spectrometry (GC-MS 7890A-5975C, United States) for quantitative analysis. The instrument condition and parameters settings were not reiterated here. Full scan mode of GC-MS was employed and the intermediates generated were distinguished the by the ChemStation library. According to the relative response area compared with the internal standard, the quantitative and semi-quantitative analysis of PAHs were undertaken. The detection limit of FLU was 0.0029 ug ml^{-1} and the average recovery were between 87.36.

To investigate the variation of functional groups, the Fourier transform infrared (FTIR) spectra of the HA in HA/Fe (II)/PS system over time were obtained by an infrared spectrometer (Frontier FT-IR, United States). The test parameters were set as follows: wave number range: 4000–400 cm^{-1}; scan times: 32; resolution ratio: 4 cm^{-1}; sample thickness: 10–50 um.

Short-lived intermediates include a variety of free radical adducts were observed by an electron paramagnetic resonance (EPR) spectrometer (E-500, BRUKER, Germany). The free radicals adduct generated from the capture of 5,5-dimethyl-1-pyrroline N-oxide (DMPO), then they were collected at selected intervals and tested by means of electron spin resonance (ESR) technique.

The instrument conditions of ESR were set as follows: sweep width, 100 G; modulation amplitude, 3.08 G; a resonance frequency, 9.75 GHz; time constant, 10.24 ms; conversion time, 20.48 ms.

Results and discussion

Degradation kinetics and radical identification for HA/Fe (II)/PS system

To verify the feasibility of PS activated by HA, the performance of various activation ways of PS for FLU degradation was investigated. The elimination of FLU directly demonstrated the PS activation performance. As shown in Figure 1A, the concentrations of FLU presented a continuous downward trend after degradation. The largest loss in FLU yields was observed in HA/Fe (II)/PS system, which had reached 98% after 24 h. While separately 66% or 92% of FLU was degraded by Fe (II)/PS and HA/PS. The findings revealed that HA had significant synergistic effects on Fe (II) activated PS process (Zhang et al., 2022). The EPR spectra of free radicals generated in various systems were presented in Figure 1B. As we know, hydroxyl radical (OH) and $SO_4^{\cdot-}$ made a decisive contribution to the successful degradation of the organic pollutant in PS oxidation (Tsitonaki et al., 2010; Yuan et al., 2011; Zeng et al., 2015; Zeng et al., 2016; Lee et al., 2020). Apart from the above free radicals, semiquinone radical ($SQ^{\cdot-}$) was also detected in the presence of BQ. Besides, the intensity of OH·, $SO_4^{\cdot-}$, and $SQ^{\cdot-}$ were significantly enhanced when introduced BQ into the reaction system, especially for the HA/Fe (II)/PS system. The results were consistent with the kinetic experiments. Result had reported that carbon-based catalyst exhibited an excellent performance on persulfate activation, primarily relay on OH and $SO_4^{\cdot-}$ (Luo et al., 2020; Li et al., 2022). This might be attributed to the rich porous structure, huge surface area and abundant functional groups of HA, which could benefit the formation of countless bonding sites (Hung et al., 2022; Xu et al., 2022; Yao et al., 2022). The existence of functional groups in HA, especially quinones, was considered to be an important factor in PS activation (Fang et al., 2013; Zhang et al., 2021).

Identification of functional groups in HA

To explore the leading functional groups which take responsible for FLU degradation, FTIR spectra of HA were obtained at different reaction time with the region from 4000 to 500 cm^{-1} (Figure 2). The absorption peaks at 3415 cm^{-1} gradually decreased along with the prolonged time (0–7 days), that might be ascribed to N-H stretching vibration or O-H stretching (Li et al., 2022; Zhang et al., 2022). The prominent peak at 1612 cm^{-1} was attributed to asymmetric stretching of ionized carboxyl groups and aromatic C=C, C=O of quinone or H-bonded conjugated ketones (Ghosh et al., 2009;

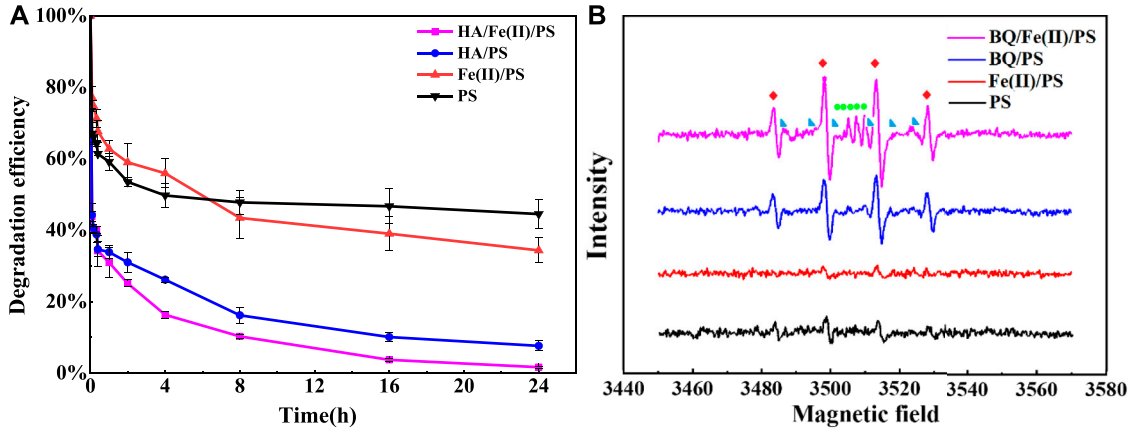

FIGURE 1
(A) Degradation kinetics of FLU under various activation conditions; **(B)** EPR spectra for the detection of PS, Fe (II)/PS, HA/PS and HA/Fe (II)/PS system. Conditions: $[PS]_0$ = 5 mM, $[BQ]_0$ = $[PS]_0$ = 0.2 mM,◆DMPO-OH,◣: DMPO-SO4, ●: SQ·-.

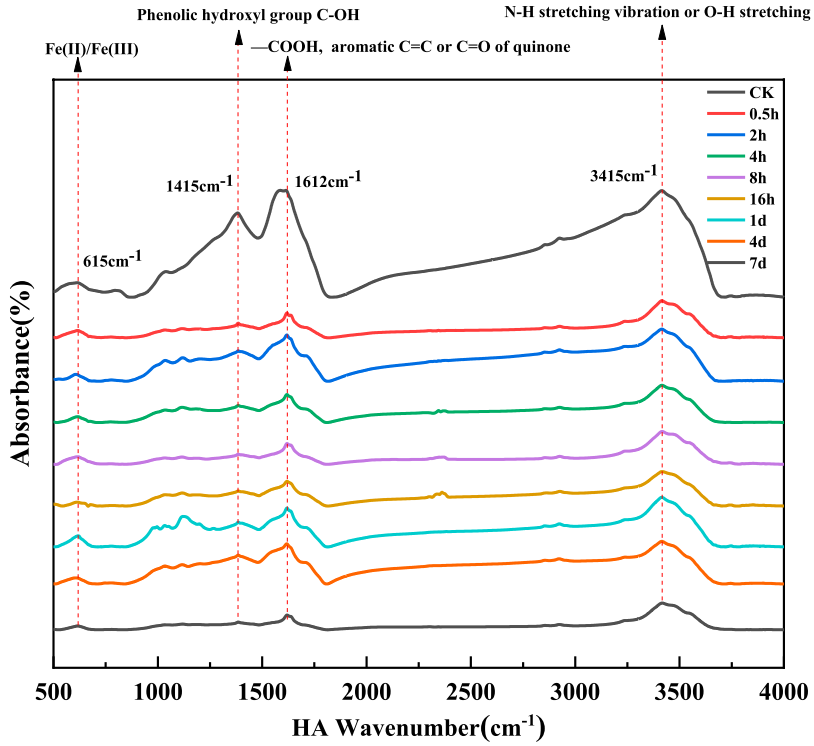

FIGURE 2
FTIR spectrum of HA samples at different reaction time.

Yao et al., 2022). The peaks of the hydroxyl group showed the same pattern as the quinone group, which indicated HA played an active role in the production of hydroxyl radicals. A band around 1415 cm^{-1} had been assigned to the C-OH stretching of phenolic hydroxyl. Studies had shown that phenolic hydroxyl was the main group to reduce Cr(VI) into Cr(III) and generate

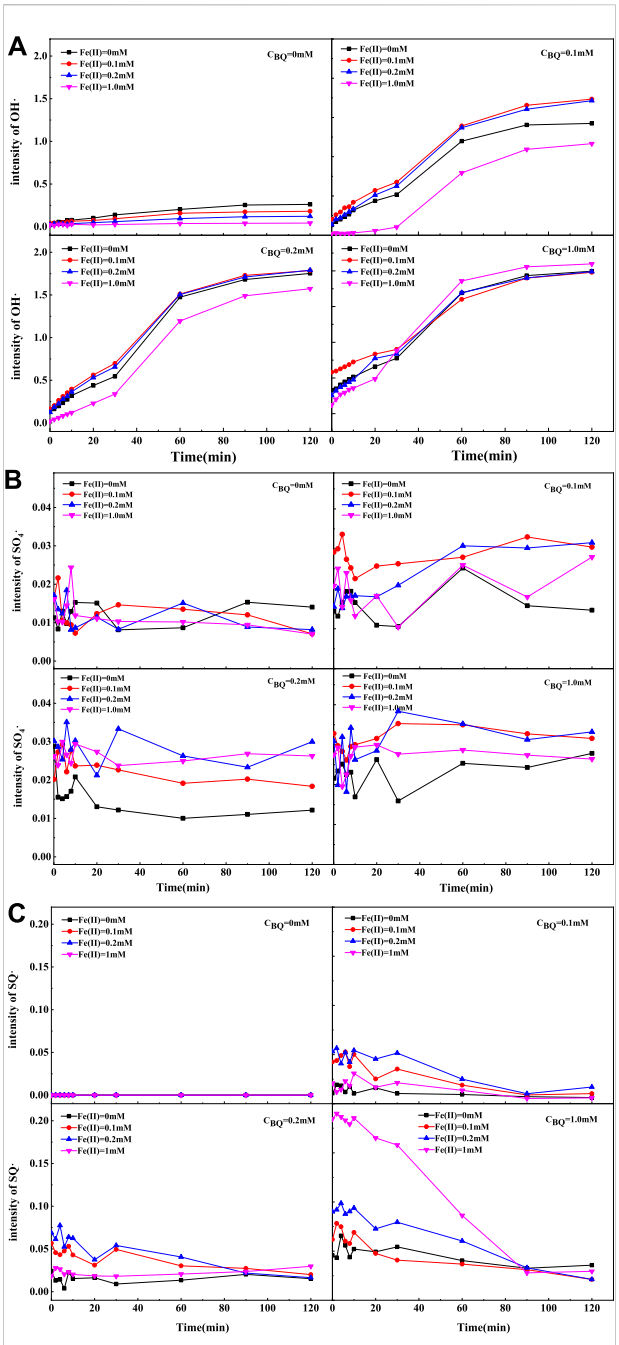

FIGURE 3
The response intensity of free radicals in BQ/Fe (II)/PS system with DMPO spin trapping agent: **(A)** OH·, **(B)** $SO_4^{\cdot-}$, **(C)** $SQ^{\cdot-}$.

carbonyl and carboxyl groups as well (Hsu et al., 2009). As the decline of carboxylic groups, the peaks at 1380 cm^{-1} presented decreased, which were assigned to O-H bending deformation of carboxylic groups, C-O stretching of phenolic groups or C-H deformation (Monda et al., 2017; Zhang et al., 2017). The small peak at 615 cm^{-1} might be caused by the presence of a large number of iron ions in the reaction system (Yao et al., 2022). The results indicated that the carboxylic, phenolic, hydroxyl, quinone groups were the dominant groups which involved in the electron transfer and oxidation-reduction reactions.

Effect of the dosages of BQ and Fe (II) on the production of free radicals

The dosages and proportions of various activators were crucial for degrading toxic recalcitrant organic pollutants (Zhang et al., 2022). To further explore the enhancement of BQ on activation, the orthogonal experiments were designed to figure out the optimum conditions in terms of the concentration of BQ and Fe (II). The production of free radicals under various conditions were displayed in Figure 3. In general, the response intensity of free radicals was strongly affected by the BQ/Fe (II) molar ratio.

Figure 3A indicated that OH intensity significantly enhanced when introduced BQ into Fe (II)/PS system. The results demonstrated that the intensity of OH increased as the reaction time extending. There continues to be a gradual decline of OH with the increasing concentration of Fe(II) when BQ concentration was 0 mm. At the given initial concentration of BQ (0.1 and 0.2 mm), the intensity of OH presented a slow increase followed by a rapid decrease. The highest catalytic activity of OH was exhibited when BQ concentration was 0.1 and 0.2 mm, respectively. When the concentration of BQ was 1.0 mm, the intensity of OH increased gradually as Fe(II) concentration rose, and reached the maximum at 1.0 mm. Basically, the yield of OH will decline once the proportion of Fe(II)/BQ exceeds 1. The most OH was produced at the same concentration of BQ and Fe(II).

The intensity of $SO_4^{\cdot-}$ was described in Figure 3B. It had demonstrated that BQ could coordinate with Fe(II) to promote more $SO_4^{\cdot-}$ production. Moreover, there was no distinct difference among all the treatments without BQ. When BQ was added, the intensity of $SO_4^{\cdot-}$ improved obviously. The most significant enhancement generally happened when the BQ concentration was in the range of 0.1–0.2 mm. The catalytic activity of $SO_4^{\cdot-}$ seemed to decline due to an excessive amount of BQ and Fe (II), which might be due to the competitive effect of Fe (II) on $SO_4^{\cdot-}$ (Dominguez et al., 2019).

The variation of $SQ^{\cdot-}$ in different systems was exhibited in Figure 3C. There was evidence that $SQ^{\cdot-}$ could not generate in the absence of BQ. Besides, the intensity of $SQ^{\cdot-}$ had decreased markedly over time, which differed from the variation of OH and $SO_4^{\cdot-}$. With the content of BQ fixed, the order of $SQ^{\cdot-}$ intensity was similar to that of OH·. When the concentration of BQ was in the range of 0.1–0.2 mm, the variation of $SQ^{\cdot-}$ intensity with Fe(II) concentration increased first, and then decreased. While as the BQ concentration rose to 1.0 mM, the intensity of $SQ^{\cdot-}$ was significantly strengthened with the increase

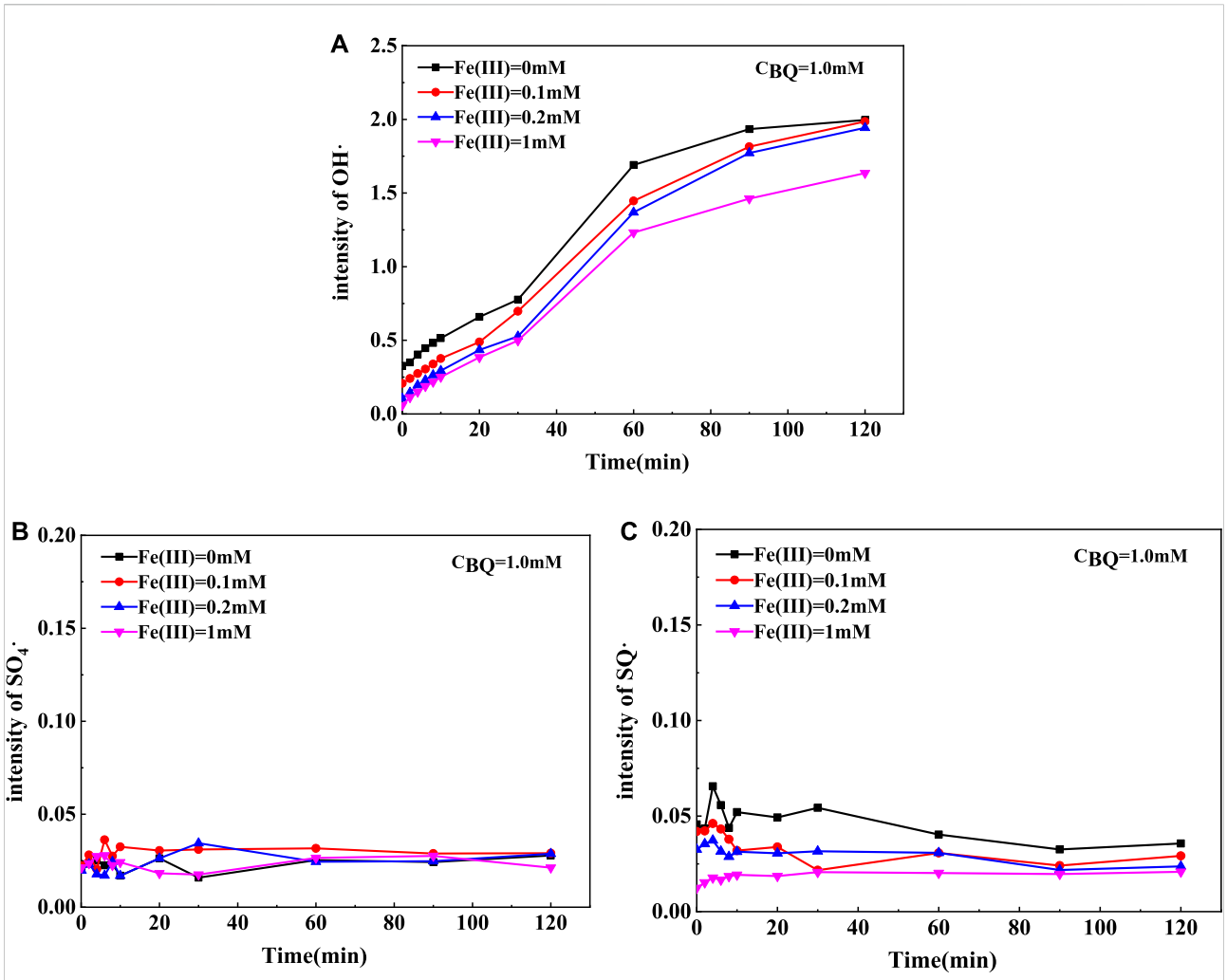

FIGURE 4
The response intensity of free radicals in BQ/Fe (III)/PS system with DMPO spin trapping agent: **(A)** OH·, **(B)** SO_4·$^-$, **(C)** SQ·$^-$.

of Fe(II) concentration. The maximum SQ·$^-$ was usually produced at the same concentration of BQ and Fe(II).

The catalytic performance had been greatly enhanced by quinone groups. Specifically, as the BQ concentration increased, the response intensity of SQ·$^-$ and OH had strengthened rapidly. Without BQ, Fe (II) had an inhibitory effect on hydroxyl radicals, which might be caused by the unproductive consumption of OH from Fe(II) (Wang et al., 2020). The moderate level of quinones could reduce the unproductive consumption of PS, while excessive dosage could grab SO_4·$^-$ and OH from the system. Quinone could affect directly on the production of active species, which was attributed to the electron shuttles action during chemical processes (Aeschbacher et al., 2012; Zhang et al., 2021). The preliminary study noted that there might be Fe(II)/Fe(III) and semiquinone/quinone cycle in the catalyzed oxidation system (Leng et al., 2014; Li et al., 2022). In conclusion, the addition of an appropriate amount of Fe (II) and quinone could promote the decomposition of PS and the generation of free radicals to attack FLU. In this study, we had confirmed the optimizing ratio of Fe (II) and BQ was 1:1, which demonstrated a superior performance on FLU degradation.

Effect of the dosages of BQ and Fe (III) on the production of free radicals

To further prove the effect of iron in various valence on the degradation characteristic, the interaction between Fe (III) and BQ was investigated (see Figure 4). According to the previous results, the study was conducted with 1.0 mM BQ. In contrast, the intensity of free radicals was restrained in the co-existence of HA and Fe (III), revealing that Fe (III) had inhibited the activation process. Specifically, the intensity of OH and SQ·$^-$ gradually reduced with the increase of Fe(III)

TABLE 1 Identification of degradation components in inactivated and activated PS systems.

Products	Specific for inactivated system	Co-occurrences for both	Specific for activated system
Hydro-carbon	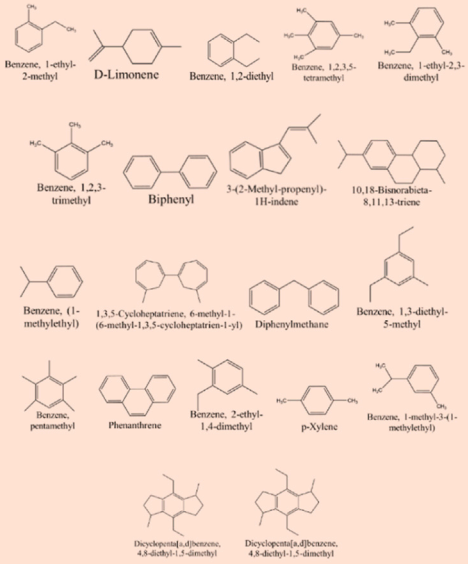		
-O	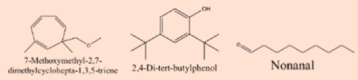		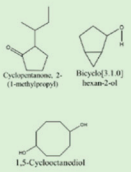
-Si			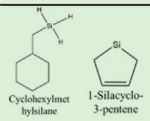
-S		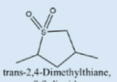	
-Cl			
-F		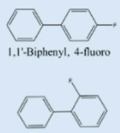	

concentration. The intensity of $SQ\cdot^-$ reached the maximum within 2–4 min, then decreased sharply and tended to be flat after 10 min. It might be due to the decomposition of persulfate and the generation of free redicals decelerated. The more Fe (Ⅲ) we added, the effect of antagonism was more abvious. By contrast, there was little variation in $SO_4^{\cdot-}$. It might be caused by the reversible reaction between Fe(II)/Fe(III) and $SQ\cdot^-/Q\cdot^-$, which promote the formation of more $SO_4^{\cdot-}$in the system (Fang et al., 2013). Besides, excessive Fe(III) would diminish the reduction capacity and electron

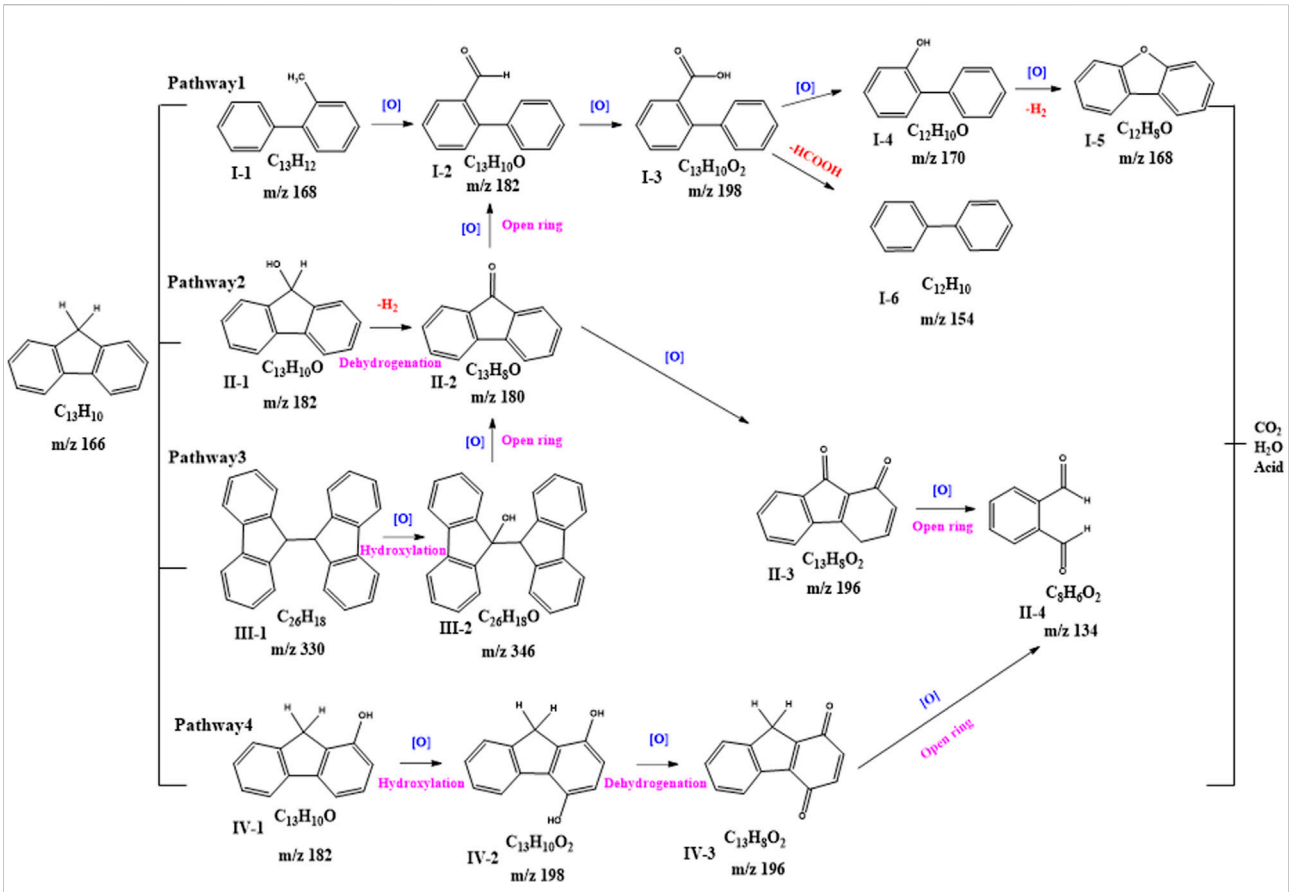

FIGURE 5
Proposed FLU degradation pathways in HA/Fe (II)/PS system.

transfer process, resulting in low generation of free radicals and poor degradation efficiency.

Degradation mechanisms and pathway

The degradation of PAHs usually resulted in ring-opening and forming some oxidized intermediates. To further verify the risk in HA/Fe (II)/PS system, generated by-products were discerned by electron ionization mass spectrometry (EI-MS). The degradation components of FLU in inactivated and activated PS systems in contaminated soil were summarized in Table 1. In this study, the oxidized intermediates of FLU contained furan, phenol, ketone, thiophene and aromatic derivatives, *etc.* Among them, Polar PAHs had higher toxicity than nonpolar PAHs because of their high mobility and bioavailability (Lundstedt et al., 2007; Cai et al., 2017; Idowu et al., 2019). However, polar PAHs are not included in the Monitoring list of the United States Environmental Protection Agency (USEPA), indicating that the environmental risk might be seriously underrated (Witter and Nguyen 2016). Compared to the inactivated system, the degradation component had fallen from 31 to 13, indicating an even lower risk in practical application.

According to the EI-MS analysis results, four conceivable degradation pathways of FLU in HA/Fe (II)/PS system were proposed (Figure 5). The crutial routes of reactions involved decarboxylation, oxidative dehydrogenation, hydroxylation and ring-opening, which resulted in the formation of oxidized intermediate including phenols, furans, ketones, aldehydes. In pathway I, product I-3 (m/z = 198) was produced by the ring-opening and gradual oxidization. Subsequently, product I-3 was further transformed to product I-6 (m/z = 154) by decarboxylation, or oxidized to product I-5 (m/z = 168). In pathway II and III, fluorenone (m/z = 180) was an important intermediate that should be a matter of concern. Phthalic aldehyde (m/z = 134) was identified as the products of multistage oxidation. Phthalic aldehyde (m/z = 134) was also generated *via* hydroxylation, oxidative dehydrogenation and ring-opening process in pathway IV. Finally, the by-products were transformed into small molecule material and further oxidized to H_2O and CO_2^-, *etc.*

Conclusion

In this study, HA/Fe (II)/PS has been verified as an effective method for FLU degradation. HA is attractive material characterized by renewable, low-cost and environmental-friendly. The findings of this work provide new insights into the degradation of PAHs and a certain basis for the remediation of organic contaminated sites. The main conclusions are summarized as follows.

(1) HA/Fe (II)/PS achieved the best performance in FLU degradation, and OH·, $SO_4^{\cdot-}$ and $SQ^{\cdot-}$ were observed by EPR experiment.
(2) The combination of BQ/Fe (II) was endowed with a synergistic effect, while the presence of Fe (III) restrained PS activation by BQ. The optimum proportion of BQ/Fe (II) had been identified as 1:1.
(3) Significantly, $SQ^{\cdot-}$ was the dominant active specie that could stimulate PS decomposition and the generation of free radicals to attack FLU. The oxidation involved decarboxylation, oxidative dehydrogenation, hydroxylation and ring-opening, resulting a decline in the variety and toxicity of degradation components.

Data availability statement

The original contributions presented in the study are included in the article/Supplementary Material, further inquiries can be directed to the corresponding author.

Author contributions

HL: Investigation, Writing—original draft. XL: Conceptualization, Writing—review and editing, Supervision. YL: Methodology, Writing, review and editing, Supervision, Project administration. QL: Data processing, Visualization JL: Investigation, Methodology.

Funding

This study was financially supported by the National Nature Science Foundation of China (Grant No. 42007129, 42225707) and the Strategic Priority Research Program of the Chinese Academy of Sciences (XDA23010400).

Conflict of interest

The authors declare that the research was conducted in the absence of any commercial or financial relationships that could be construed as a potential conflict of interest.

Publisher's note

All claims expressed in this article are solely those of the authors and do not necessarily represent those of their affiliated organizations, or those of the publisher, the editors and the reviewers. Any product that may be evaluated in this article, or claim that may be made by its manufacturer, is not guaranteed or endorsed by the publisher.

References

Aeschbacher, M., Graf, C., Schwarzenbach, R. P., and Sander, M. (2012). Antioxidant properties of humic substances. *Environ. Sci. Technol.* 46 (9), 4916–4925. doi:10.1021/es300039h

Cai, C. Y., Li, J. Y., Di, W., Wang, X. L., Tsang, D. C. W., and Li, X. D. (2017). Spatial distribution, emission source and health risk of parent PAHs and derivatives in surface soils from the Yangtze River Delta, eastern China. *Chemosphere* 178, 301–308. doi:10.1016/j.chemosphere.2017.03.057

Ding, Z. Z., Yi, Y. Y., Zhang, Q. Z., and Zhuang, T. (2019). Theoretical investigation on atmospheric oxidation of fluorene initiated by OH radical. *Sci. Total Environ.* 669, 920–929. doi:10.1016/j.scitotenv.2019.02.400

Dominguez, C. M., Rodriguez, V., Montero, E., Romero, A., and Santos, A. (2019). Methanol-enhanced degradation of carbon tetrachloride by alkaline activation of persulfate: Kinetic model. *Sci. Total Environ.* 666, 631–640. doi:10.1016/j.scitotenv.2019.02.223

Dong, C. D., Chen, C. W., and Hung, C. M. (2017). Synthesis of magnetic biochar from bamboo biomass to activate persulfate for the removal of polycyclic aromatic hydrocarbons in marine sediments. *Bioresour. Technol.* 245, 188–195. doi:10.1016/j.biortech.2017.08.204

Drwal, E., Rak, A., and Gregoraszczuk, E. L. (2019). Review: Polycyclic aromatic hydrocarbons (PAHs)-Action on placental function and health risks in future life of newborns. *Toxicology* 411, 133–142. doi:10.1016/j.tox.2018.10.003

Duesteberg, C. K., and Waite, T. D. (2007). Kinetic modeling of the oxidation of p-hydroxybenzoic acid by Fenton's reagent: Implications of the role of quinones in the redox cycling of iron. *Environ. Sci. Technol.* 41 (11), 4103–4110. doi:10.1021/es0628699

Fang, G. D., Gao, J., Dionysiou, D. D., Liu, C., and Zhou, D. M. (2013). Activation of persulfate by quinones: Free radical reactions and implication for the degradation of PCBs. *Environ. Sci. Technol.* 47 (9), 4605–4611. doi:10.1021/es400262n

Garcia-Cervilla, R., Santos, A., Romero, A., and Lorenzo, D. (2022). Abatement of chlorobenzenes in aqueous phase by persulfate activated by alkali enhanced by surfactant addition. *J. Environ. Manage.* 306, 114475. doi:10.1016/j.jenvman.2022.114475

Ghosh, S., Wang, Z. Y., Kang, S., Bhowmik, P. C., and Xing, B. S. (2009). Sorption and fractionation of a peat derived humic acid by kaolinite, montmorillonite, and goethite. *Pedosphere* 19 (1), 21–30. doi:10.1016/s1002-0160(08)60080-6

Hayakawa, K. (2016). Environmental behaviors and toxicities of polycyclic aromatic hydrocarbons and nitropolycyclic aromatic hydrocarbons. *Chem. Pharm. Bull.* 64 (2), 83–94. doi:10.1248/cpb.c15-00801

Hsu, N. H., Wang, S. L., Lin, Y. C., Sheng, G. D., and Lee, J. F. (2009). Reduction of Cr(VI) by crop-residue-derived black carbon. *Environ. Sci. Technol.* 43 (23), 8801–8806. doi:10.1021/es901872x

Hung, C. M., Chen, C. W., Huang, C. P., and Dong, C. D. (2022). Removal of 4-nonylphenol in activated sludge by peroxymonosulfate activated with sorghum distillery residue-derived biochar. *Bioresour. Technol.* 360, 127564. doi:10.1016/j.biortech.2022.127564

Idowu, O., Semple, K. T., Ramadass, K., O'Connor, W., Hansbro, P., and Thavamani, P. (2019). Beyond the obvious: Environmental health implications of polar polycyclic aromatic hydrocarbons. *Environ. Int.* 123, 543–557. doi:10.1016/j.envint.2018.12.051

Kang, S. H., and Choi, W. (2009). Oxidative degradation of organic compounds using zero-valent iron in the presence of natural organic matter serving as an electron shuttle. *Environ. Sci. Technol.* 43 (3), 878–883. doi:10.1021/es801705f

Lee, J., von Gunten, U., and Kim, J. H. (2020). Persulfate-based advanced oxidation: Critical assessment of opportunities and roadblocks. *Environ. Sci. Technol.* 54 (6), 3064–3081. doi:10.1021/acs.est.9b07082

Leng, Y. Q., Guo, W. L., Shi, X., Li, Y. Y., Wang, A. Q., and Hao, F. F. (2014). Degradation of Rhodamine B by persulfate activated with Fe3O4: Effect of polyhydroquinone serving as an electron shuttle. *Chem. Eng. J.* 240, 338–343. doi:10.1016/j.cej.2013.11.090

Li, B. Z., Li, L., Lin, K. F., Zhang, W., Lu, S. G., and Luo, Q. S. (2013). Removal of 1, 1, 1-trichloroethane from aqueous solution by a sono-activated persulfate process. *Ultrason. Sonochem.* 20 (3), 855–863. doi:10.1016/j.ultsonch.2012.11.014

Li, Q., Tang, Y., Zhou, B., Zhou, J., and Shi, B. (2022). Resource utilization of tannery sludge to prepare biochar as persulfate activators for highly efficient degradation of tetracycline. *Bioresour. Technol.* 358, 127417. doi:10.1016/j.biortech.2022.127417

Li, W., Orozco, R., Camargos, N., and Liu, H. Z. (2017). Mechanisms on the impacts of alkalinity, pH, and chloride on persulfate-based groundwater remediation. *Environ. Sci. Technol.* 51 (7), 3948–3959. doi:10.1021/acs.est.6b04849

Li, X. D., Wu, B., Zhang, Q., Xu, D. P., Liu, Y. Q., and Ma, F. J. (2019). Mechanisms on the impacts of humic acids on persulfate/Fe^{2+}-based groundwater remediation. *Chem. Eng. J.* 378, 122142. doi:10.1016/j.cej.2019.122142

Liu, G. S., You, S. J., Tan, Y., and Ren, N. Q. (2017). *In situ* photochemical activation of sulfate for enhanced degradation of organic pollutants in water. *Environ. Sci. Technol.* 51 (4), 2339–2346. doi:10.1021/acs.est.6b05090

Liu, Y. K., Zhang, Y., Wang, B. J., Wang, S. Y., Liu, M., and Wu, Y. L. (2020). Degradation of ibuprofen in soil systems by persulfate activated with pyrophosphate chelated Fe(II). *Chem. Eng. J.* 379, 122145. doi:10.1016/j.cej.2019.122145

Liu, Z., Pan, S., Xu, F., Wang, Z., Zhao, C., and Xu, X. (2022). Revealing the fundamental role of MoO2 in promoting efficient and stable activation of persulfate by iron carbon based catalysts: Efficient Fe^{2+}/Fe^{3+} cycling to generate reactive species. *Water Res.* 225, 119142. doi:10.1016/j.watres.2022.119142

Lundstedt, S., White, P. A., Lemieux, C. L., Lynes, K. D., Lambert, L. B., and Oberg, L. (2007). Sources, fate, and toxic hazards of oxygenated polycyclic aromatic hydrocarbons (PAHs) at PAH-contaminated sites. *AMBIO A J. Hum. Environ.* 36 (6), 475–485. doi:10.1579/0044-7447(2007)36[475:sfatho]2.0.co;2

Luo, J., Zhu, Y., Zhang, Q., Cao, M., Guo, W., and Li, H. (2020). Promotion of short-chain fatty acids production and fermented sludge properties via persulfate treatments with different activators: Performance and mechanisms. *Bioresour. Technol.* 295, 122278. doi:10.1016/j.biortech.2019.122278

Monda, H., Cozzolino, V., Vinci, G., Spaccini, R., and Piccolo, A. (2017). Molecular characteristics of water-extractable organic matter from different composted biomasses and their effects on seed germination and early growth of maize. *Sci. Total Environ.* 590, 40–49. doi:10.1016/j.scitotenv.2017.03.026

Nam, T. H., Jeon, H. J., Mo, H., Cho, K., Ok, Y. S., and Lee, S. E. (2015). Determination of biomarkers for polycyclic aromatic hydrocarbons (PAHs) toxicity to earthworm (*Eisenia fetida*). *Environ. Geochem. Health* 37 (6), 943–951. doi:10.1007/s10653-015-9706-z

Qi, C., Liu, X., Ma, J., Lin, C., Li, X., and Zhang, H. (2016). Activation of peroxymonosulfate by base: Implications for the degradation of organic pollutants. *Chemosphere* 151, 280–288. doi:10.1016/j.chemosphere.2016.02.089

Rombola, A. G., Meredith, W., Snape, C. E., Baronti, S., Genesio, L., and Vaccari, F. P. (2015). Fate of soil organic carbon and polycyclic aromatic hydrocarbons in a vineyard soil treated with biochar. *Environ. Sci. Technol.* 49 (18), 11037–11044. doi:10.1021/acs.est.5b02562

Sun, B., Ma, J., and Sedlak, D. L. (2016). Chemisorption of perfluorooctanoic acid on powdered activated carbon initiated by persulfate in aqueous solution. *Environ. Sci. Technol.* 50 (14), 7618–7624. doi:10.1021/acs.est.6b00411

Tsitonaki, A., Petri, B., Crimi, M., Mosbaek, H., Siegrist, R. L., and Bjerg, P. L. (2010). *In situ* chemical oxidation of contaminated soil and groundwater using persulfate: A review. *Crit. Rev. Environ. Sci. Technol.* 40 (1), 55–91. doi:10.1080/10643380802039303

Wang, L., Peng, L. B., Xie, L. L., Deng, P. Y., and Deng, D. Y. (2017). Compatibility of surfactants. And thermally activated persulfate for enhanced subsurface remediation. *Environ. Sci. Technol.* 51 (12), 7055–7064. doi:10.1021/acs.est.6b05477

Wang, L., Wu, H. H., and Deng, D. Y. (2020). Role of surfactants in accelerating or retarding persulfate decomposition. *Chem. Eng. J.* 384, 123303. doi:10.1016/j.cej.2019.123303

Westerhoff, P., Mezyk, S. P., Cooper, W. J., and Minakata, D. (2007). Electron pulse radiolysis determination of hydroxyl radical rate constants with Suwannee river fulvic acid and other dissolved organic matter isolates. *Environ. Sci. Technol.* 41 (13), 4640–4646. doi:10.1021/es062529n

Witter, A. E., and Nguyen, M. H. (2016). Determination of oxygen, nitrogen, and sulfur-containing polycyclic aromatic hydrocarbons (PAHs) in urban stream sediments. *Environ. Pollut.* 209, 186–196. doi:10.1016/j.envpol.2015.10.037

Xiao, S., Cheng, M., Zhong, H., Liu, Z. F., Liu, Y., and Yang, X. (2020). Iron-mediated activation of persulfate and peroxymonosulfate in both homogeneous and heterogeneous ways: A review. *Chem. Eng. J.* 384, 123265. doi:10.1016/j.cej.2019.123265

Xu, Z. M., Li, R. H., Wu, S. H., He, Q. F., Ling, Z. M., and Liu, T. (2022). Cattle manure compost humification process by inoculation ammonia-oxidizing bacteria. *Bioresour. Technol.* 344, 126314. doi:10.1016/j.biortech.2021.126314

Yao, B., Luo, Z. R., Du, S. Z., Yang, J., Zhi, D., and Zhou, Y. Y. (2022). Magnetic MgFe2O4/biochar derived from pomelo peel as a persulfate activator for levofloxacin degradation: Effects and mechanistic consideration. *Bioresour. Technol.* 346, 126547. doi:10.1016/j.biortech.2021.126547

Yousefi, N., Pourfadakari, S., Esmaeili, S., and Babaei, A. A. (2019). Mineralization of high saline petrochemical wastewater using Sonoelectro-activated persulfate: Degradation mechanisms and reaction kinetics. *Microchem. J.* 147, 1075–1082. doi:10.1016/j.microc.2019.04.020

Yuan, R. X., Ramjaun, S. N., Wang, Z. H., and Liu, J. S. (2011). Effects of chloride ion on degradation of Acid Orange 7 by sulfate radical-based advanced oxidation process: Implications for formation of chlorinated aromatic compounds. *J. Hazard. Mat.* 196, 173–179. doi:10.1016/j.jhazmat.2011.09.007

Zeng, H. B., Liu, S. S., Chai, B. Y., Cao, D., Wang, Y., and Zhao, X. (2016). Enhanced photoelectrocatalytic decomplexation of Cu-edta and Cu recovery by persulfate activated by UV and cathodic reduction. *Environ. Sci. Technol.* 50 (12), 6459–6466. doi:10.1021/acs.est.6b00632

Zeng, T., Zhang, X. L., Wang, S. H., Niu, H. Y., and Cai, Y. Q. (2015). Spatial confinement of a Co_3O_4 catalyst in hollow metal-organic frameworks as a nanoreactor for improved degradation of organic pollutants. *Environ. Sci. Technol.* 49 (4), 2350–2357. doi:10.1021/es505014z

Zhang, J., Chen, L. P., Yin, H. L., Jin, S., Liu, F., and Chen, H. H. (2017). Mechanism study of humic acid functional groups for Cr(VI) retention: Two-dimensional FTIR and 13C CP/MAS NMR correlation spectroscopic analysis. *Environ. Pollut.* 225, 86–92. doi:10.1016/j.envpol.2017.03.047

Zhang, X., Yang, Y., Ngo, H. H., Guo, W., Sun, F., and Wang, X. (2022). Urea removal in reclaimed water used for ultrapure water production by spent coffee biochar/granular activated carbon activating peroxymonosulfate and peroxydisulfate. *Bioresour. Technol.* 343, 126062. doi:10.1016/j.biortech.2021.126062

Zhang, Y., Xu, M., Liu, X., Wang, M., Zhao, J., and Li, S. (2021). Regulation of biochar mediated catalytic degradation of quinolone antibiotics: Important role of environmentally persistent free radicals. *Bioresour. Technol.* 326, 124780. doi:10.1016/j.biortech.2021.124780

Zhou, S. Q., Yu, Y. H., Zhang, W. Q., Meng, X. Y., Luo, J. M., and Deng, L. (2018). Oxidation of microcystin-LR via activation of peroxymonosulfate using ascorbic acid: Kinetic modeling and toxicity assessment. *Environ. Sci. Technol.* 52 (7), 4305–4312. doi:10.1021/acs.est.7b06560

Zhou, Z., Liu, X., Sun, K., Lin, C., Ma, J., and He, M. (2019). Persulfate-based advanced oxidation processes (AOPs) for organic-contaminated soil remediation: A review. *Chem. Eng. J.* 372, 836–851. doi:10.1016/j.cej.2019.04.213